doi: https://doi.org/10.2514/6.2017-3067

Integrated Sizing and Multi-objective Optimization of Aircraft and Subsystem Architectures in Early Design

Dushhyanth Rajaram*, Yu Cai*, Imon Chakraborty†, Tejas G. Puranik*
and Dimitri N. Mavris‡
Aerospace Systems Design Laboratory, Georgia Institute of Technology, Atlanta, Georgia, 30332-0150

The aerospace industry's current trend towards novel or More Electric architectures results in some unique challenges for designers due to both a scarcity or absence of historical data and a potentially large combinatorial space of possible architectures. These add to the already existing challenges of attempting to optimize an aircraft design in the presence of multiple possible objective functions while avoiding an overly compartmentalized approach. This paper uses the Integrated Subsystem Sizing and Architecture Assessment Capability to pursue a multi-objective optimization for a Large Twin-aisle Aircraft and a Small Single-aisle Aircraft using the Non-dominated Sorting Genetic Algorithm II with parallel function evaluations. One novelty of the optimization setup is that it explicitly considers the impacts of subsystem architectures in addition to those of traditional aircraft-level design variables. The optimization yielded generations of non-dominated designs in which substantially electrified subsystem architectures were found to predominate. As a first assessment of the impact of epistemic uncertainty on the results obtained, the optimization was re-run with altered sensitivities for the thrust-specific fuel consumption penalties due to shaft-power and bleed air extraction. This analysis demonstrated that the composition of architectures on the Pareto frontier is sensitive to the secondary power extraction penalties, but more so for the Small Single-aisle Aircraft than the Large Twin-aisle Aircraft.

I. Introduction

The goal of the aircraft sizing task is to use relevant point performance and mission performance requirements to iteratively arrive at a converged solution where the aircraft is defined by a geometric scale (typically represented by wing planform area), a propulsive scale (typically represented by rated sea-level static thrust), and the Maximum Takeoff Weight (MTOW). Thus, the early design phase is dominated by considerations of aerodynamics, propulsion, and structural weight estimation. Once feasibility of a notional aircraft concept is established, efforts may be expended towards the design optimization task, namely achieving a better or more *optimized* design, and ideally culminating in the *best* design. Such efforts typically involve posing the design problem as a mathematical optimization statement usually constrained by point performance and mission level requirements. However, the design of a complex system such as a commercial transport must ensure thoroughly adequate (if not optimal) performance with respect to multiple, often conflicting, performance objectives. While optimization of fuel consumption is an obvious objective, other common choices seen in literature[1–5] include MTOW (often used as a surrogate for cost), NO_x, CO_2 emissions, takeoff field length, specific range (a surrogate for off-design fuel economy), design range, noise margin, etc.

Due to the relevant yet often conflicting nature of these objectives, it is difficult to both identify and defend a single objective metric to optimize for. While approaches that attempt to map multiple objectives into a single weighted objective function do exist, these are limited in that the choice of weights, which directly influences the identified optima, is often somewhat subjective, if not arbitrary. A more logical solution, therefore, is to formulate the design problem as a multi-objective optimization statement, with the tacit understanding that the conflicting nature of the objectives may preclude the existence of designs that

*Graduate Researcher, Daniel Guggenheim School of Aerospace Engineering, AIAA Student Member
†Research Engineer II, Daniel Guggenheim School of Aerospace Engineering, AIAA Member
‡S.P. Langley NIA Distinguished Regents Professor, Daniel Guggenheim School of Aerospace Engineering, AIAA Fellow

are optimal with respect to all of them. In such cases, the focus shifts from searching for a single optimal design to identifying a set of *non-dominated Pareto-optimal* solutions, whose members are considered equally good, and for whom no single objective can be further improved without degradation of one or more other objectives. Naturally, the solution of a multi-objective optimization problem is more complicated than that of a single-objective one.

The complexity is further increased when one acknowledges that the architecture of the aircraft equipment systems or subsystems has a non-negligible impact on each of the above-mentioned major disciplines. The impact of aircraft subsystems has traditionally been accounted for through regression relationships based off historical data.[6–8] Such relationships were made possible mainly due to the presence of a large number of aircraft designs (spanning several decades) with fairly conventional architectures for the major subsystems: e.g., pneumatic Environmental Control System (ECS) and Ice Protection Systems (IPS), hydraulic actuation functions, and electrically powered avionics and cabin loads. However, the inevitable technology saturation of such designs and the rapidly improving state-of-the-art in power electronics and electric drives[9,10] have led to renewed interest in more electrified subsystem architectures as a potential means to obtain weight and fuel efficiency benefits. This is manifested in the emergence of *More Electric Aircraft* (MEA) such as the Boeing 787[11,12] and the Airbus A380,[13] where traditional hydraulic and pneumatic systems have been replaced or supplemented with electrical solutions.

When dealing with such MEA, the first additional challenge for the designer or analyst is the relative scarcity or complete absence of applicable historical data regarding the aircraft systems to use in early design and sizing. Compensating for this requires explicit consideration of subsystems earlier in the design phase, possibly through physics-based sizing and analysis approaches,[14–16] and accounting for the connectivity among various components within the subsystem architecture. A second additional challenge is the extremely large number of possible combinations arising from the presence of multiple feasible solutions for multiple aircraft subsystems. In fact, it was demonstrated in prior work that considering only a partial enumeration of possible design alternatives for major subsystems such as ECS, wing and nacelle IPS, and actuation functions (landing gear, wheel brakes, thrust reversers, and nose-wheel steering) can easily lead to in excess of $6.6 \cdot 10^6$ architecture combinations.[17] Even if a significantly reduced subset of these is considered (as in this work), the combinatorial problem of subsystem architectures still adds additional degrees-of-freedom (in the form of *discrete* design variables) to any optimization effort.

The optimization problem as described above lends itself well to the use of a Genetic Algorithm (GA). These are inherently able to handle discrete design variables (e.g., subsystem architecture descriptions) and explore large design spaces. Due to the presence of a small degree of randomness owing to their evolutionary nature, they are known to capture the global minimum if run indefinitely. In addition, because they do not rely on gradient information, they can handle nonlinear, discontinuous functions. This makes them especially suitable for objectives and constraints involving queries to engineering design codes where the underlying analytical set of equations may be unknown and/or complex. Due to the multi-objective nature of the design problem, the Non-dominated Sorting Genetic Algorithm II (NSGA-II)[18] is employed in this work. The NSGA-II algorithm employs a fast, non-dominated sorting approach and is able to find a better spread of solutions with better convergence near a Pareto front compared to other algorithms[19] This work employs the NSGA-II algorithm to supply aircraft-level continuous design variables and discrete subsystem-level architecture descriptor variables to the Integrated Subsystem Sizing and Architecture Assessment Capability (ISSAAC).[15,20,21] The ISSAAC framework integrates a tractable, physics-based sizing and analysis of major aircraft subsystems with the traditional aircraft sizing process in a modular manner, with a focus on novel architectures (e.g., MEA). It evaluates the candidate design's performance with regard to the objective functions and constraints and feeds this information back to the NSGA-II algorithm. The end goal of this optimization approach is to identify the characteristics of the Pareto-optimal designs, with regard to both the continuous (aircraft-level) and discrete (subsystem-level) design variables for a Large Twin-Aisle Aircraft (LTA) and a Small Single-Aisle Aircraft(SSA). In modern-day aircraft design programs, it is not uncommon for airframers to sub-contract the design of major aircraft subsystems to vendors and suppliers. Thus, while the airframers may be in a position to evaluate the effect of entirely different subsystem architectures, they may not be able to adequately address the detailed design of these subsystems. Therefore, while additional continuous design variables related to the detailed design and optimality of the subsystems clearly do exist, these are not considered within the scope of the current work.

The remainder of the paper is organized as follows, Section II gives a brief description of the characteristics of the NSGA-II algorithm which is employed in this work. Section III gives a brief summary of the ISSAAC

framework, which in this case is driven by the NSGA-II algorithm. Section IV discusses the proposed approach and the problem formulation. Section V presents and discusses the results of the optimization. Section VI concludes the paper and identifies some avenues for future work.

II. Non-dominated Sorting Genetic Algorithm II (NSGA-II)

Several algorithms exist for computing the Pareto frontier,[22–24] and popular approaches are evolutionary in nature.[18] Some popular non-evolutionary approaches include (but are not limited to) normal boundary intersection (NBI),[24] and normal constraint based methods.[22,23] These methods involve solving a set of single objective optimization problems usually involving a weighted-sum of the objectives to successively sample points on the Pareto frontier. Approaches that operate on such weighted-sum aggregates are known to be inappropriate for determining non-convex regions on the Pareto frontier, and struggle to attain an evenly spaced distribution of points.[24] The NSGA-II algorithm employed herein works much like genetic algorithms, in that it operates on a "population" of candidate designs, and successively returns populations that are non-dominated until a convergence criterion is met. Common genetic operators like cross-over (reproduction), mutation, and selection ensure that as generations progress, fitter members of the population are retained while the poorly performing members get discarded. In the multi-objective setting, a notion of existence of non-domination levels in the population, helps in the retention of the most non-dominated members as time advances. In other words, the members that are most non-dominated replace older members in the population. Constraint violations can be handled in a number of ways. In this work, constraints are handled by penalizing the dominance level of the population member in question in an adverse manner that guarantees that it does not emerge on the Pareto frontier. Another important feature of the NSGA-II algorithm that is particularly relevant to this work is the fact that it naturally lends itself to parallelization because it requires that a set of candidates be evaluated at any given point in time. This set of designs can therefore be evaluated simultaneously in parallel.

III. Integrated Subsystem Sizing and Architecture Assessment Capability (ISSAAC)

This section provides a brief summary of the main modules of ISSAAC, which are depicted in Fig. 1. For additional details, the reader is referred to prior works involving ISSAAC.[15,20,21] Given the numerous proprietary tools and methods used within the aerospace industry, the ISSAAC methodology was developed to be tool-agnostic. It requires the integration of tools possessing the following functionalities or capabilities (listed in parentheses are the tools currently used in ISSAAC):

1. Aircraft sizing and mission performance analysis (Flight Optimization System (FLOPS)[25]),
2. Propulsion cycle analysis (Numerical Propulsion System Simulation (NPSS)[26])
3. Subsystem sizing and analysis capability (MATLAB)
4. Analysis module integration and sequencing (MATLAB)

The propulsion cycle sizing and analysis tool is not currently directly embedded within ISSAAC. Instead, it is run off-line to generate engine performance data tables (engine decks) that are then used for sizing and mission performance analysis within the ISSAC framework. The main ISSAAC modules involve:

1. **Definition of design requirements:** These include the mission performance requirements (e.g., design range and payload), the point performance requirements (e.g., takeoff field length, approach speed, etc.), and the aircraft notional concept. Commercial transport designs with a conventional aft-tail and a tube-and-wing configuration are considered in this work. Analyses are performed for two vehicle sizes: Large Twin-Aisle Aircraft (LTA) and Small Single-Aisle Aircraft (SSA).
2. **Traditional aircraft & engine sizing:** Within this module, the goal is to define the aircraft in terms of a geometric scale (using, for instance, the wing planform area S_w), a propulsive scale (using the required sea-level static thrust T_{SL}), and key weights such as the takeoff gross weight W_{TO} and the empty weight W_e. The weight buildup relationships within FLOPS (and most other similar tools) are

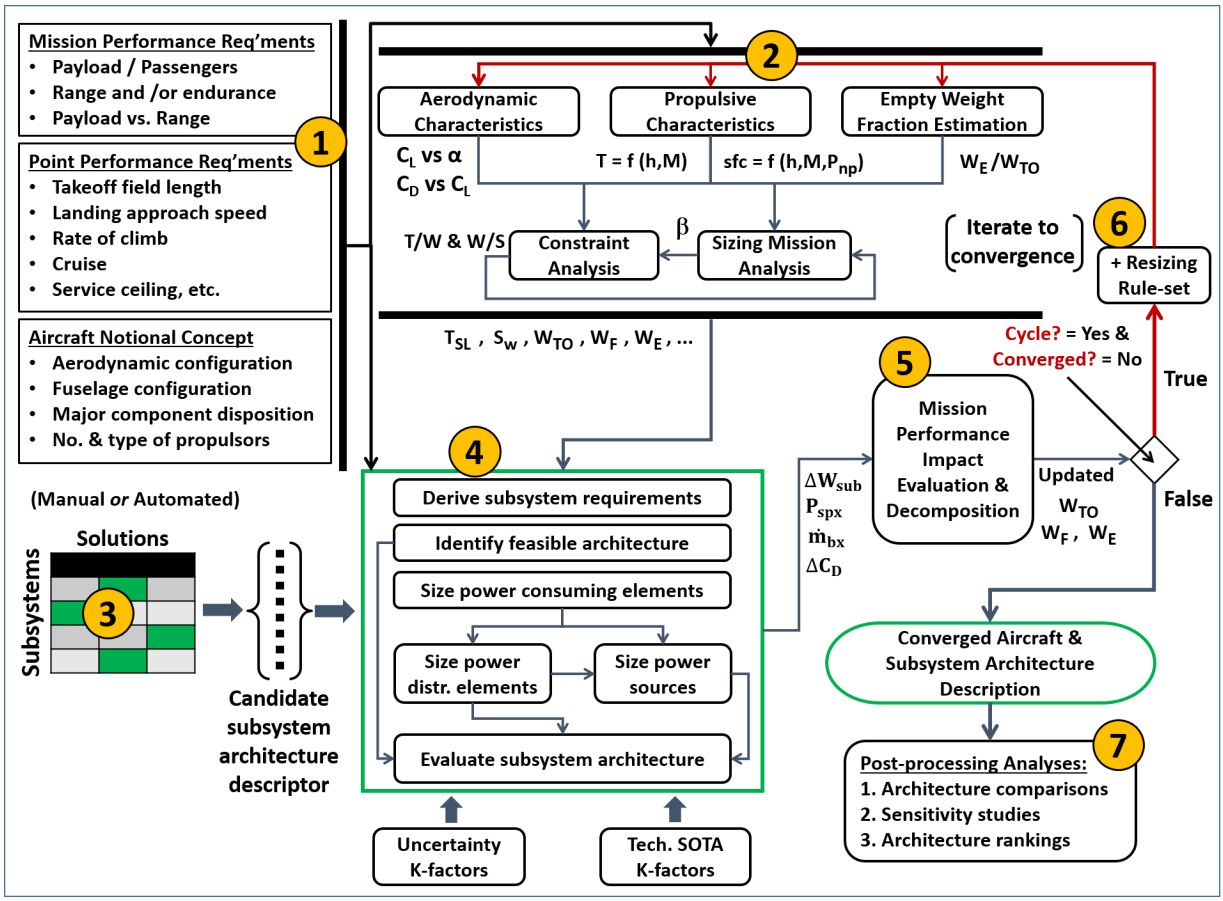

Figure 1. Main modules of Integrated Subsystem Sizing and Architecture Assessment Capability (ISSAAC)

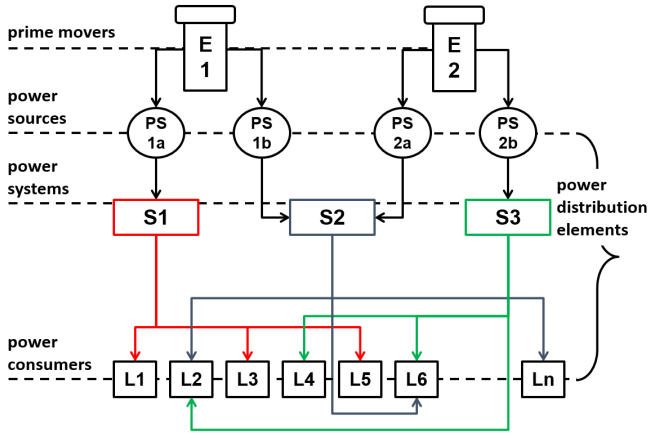

(a) Generalized representation of subsystems architecture

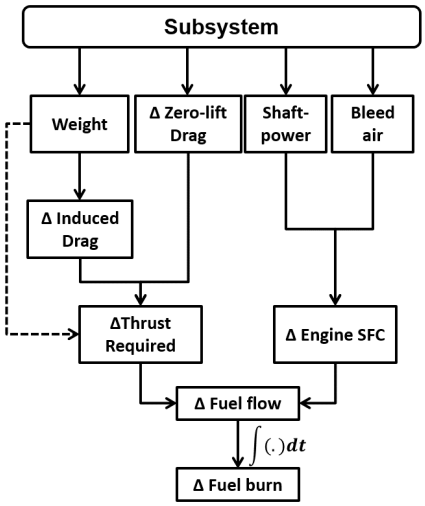

(b) Impact of subsystems on fuel consumption (mission-level metric)

Figure 2.

based on regressions of historical data, and therefore apply to conventional subsystem architectures. Thus, for the first iteration, an aircraft with conventional subsystem architecture serves as the starting point for the remaining ISSAAC modules.

3. **Candidate subsystem architecture descriptor:** This provides a qualitative description of the subsystem architecture to be evaluated in terms of the design solutions for each of the subsystems (e.g., whether the ECS is pneumatic or electric, and similar information for other subsystems).

4. **Subsystem architecture sizing and evaluation:** This module performs the sizing of the major power consuming elements, power distribution elements, and power sources within the subsystem architecture (a generalized representation of which is shown in Fig. 2(a)). The outputs of this module are the difference in weight ΔW_{sub} of the considered architecture relative to a conventional one, and time histories of the architecture's shaft-power requirement $P_{spx}(t)$, bleed air requirement $\dot{m}_{bx}(t)$, and direct drag increment $\Delta C_D(t)$. The latter three time-varying quantities are computed for each subsystem and also for the architecture as a whole.

5. **Mission performance impact evaluation and decomposition:** This module re-evaluates the impact of the subsystem architecture on the mission performance on the basis of the information generated by the previous modules. The subsystem architecture affects a mission-level metric such as fuel consumption through weight, secondary power requirements, and drag increments, as shown in Fig. 2(b). The impact of the overall architecture weight change ΔW_{sub}, the time-varying shaft-power requirement $P_{spx}(t)$, bleed air requirement $\dot{m}_{bx}(t)$, and direct drag increments $\Delta C_D(t)$ are then computed from fundamental considerations of changes in lift, drag, thrust, and fuel flow caused by these at each point within an invariant mission profile. The goal is to compute the incremental fuel weight at takeoff required on account of these three time-varying quantities. To this end, the following equation system is solved backwards in time (from landing, $k = n$ to takeoff, $k = 1$), with the intent of computing the takeoff fuel increment $\Delta W_f^{(1)}$:

$$\Delta C_L^{(k)} = \frac{\Delta W^{(k+1)}}{\left(\frac{1}{2}\rho V^2\right)^{(k)} S_w} = \frac{\Delta W_f^{(k+1)} + \Delta W_{sub}}{\left(\frac{1}{2}\rho V^2\right)^{(k)} S_w} \tag{1a}$$

$$\Delta C_{D_i}^{(k)} = C_{D_i}(C_{L,0}^{(k)} + \Delta C_L^{(k)}) - C_{D_i}(C_{L,0}^{(k)}) \tag{1b}$$

$$\Delta D_{ddl}^{(k)} = \left(\frac{1}{2}\rho V^2\right)^{(k)} S_w \; \Delta C_{D_i}^{(k)} \tag{1c}$$

$$\Delta D_{dil}^{(k)} = \left(\frac{1}{2}\rho V^2\right)^{(k)} S_w \; \Delta C_{D_0}^{(k)} \tag{1d}$$

$$\Delta D^{(k)} = \Delta D_{ddl}^{(k)} + \Delta D_{dil}^{(k)} \tag{1e}$$

$$\Delta T^{(k)} = \Delta D^{(k)} + \Delta W^{(k+1)} \left(\frac{\dot{h}}{V} + \frac{1}{g}\,\dot{V}\right)^{(k)} \tag{1f}$$

$$T^{(k)} = T_0^{(k)} + \Delta T^{(k)} \tag{1g}$$

$$\Delta \dot{w}_f^{(k)} = \dot{w}_f\left(T^{(k)}, h^{(k)}, M^{(k)}, P_{spx}^{(k)}, \dot{m}_{bx}^{(k)}\right) - \dot{w}_f\left(T_0^{(k)}, h^{(k)}, M^{(k)}, 0, 0\right) \tag{1h}$$

$$\Delta W_f^{(k)} = \Delta W_f^{(k+1)} + \Delta \dot{w}_f^{(k)} \; \Delta t^{(k)} \tag{1i}$$

$$k = k - 1, \qquad \text{and repeat sequence}$$

$$\text{Start point} : k = n - 1, \Delta W_f^{(n)} = 0$$

6. **Re-sizing of aircraft & subsystems:** This module controls the iterative re-sizing of the aircraft and its subsystems in accordance with certain re-sizing rules. In this work, regardless of the subsystem architecture being considered, the aircraft are sized to maintain a certain thrust-to-weight ratio (T_{SL}/W_{TO}) and wing loading (W_{TO}/S_w) which, within the optimization framework, are supplied by the optimizer (described in Sec. IV.A). Additional re-sizing rules are imposed by requiring that constant stabilizer volume ratios be maintained (representing invariant stability and control requirements). The geometry and weights of the re-sized vehicle and its mission performance are evaluated in FLOPS with the aforementioned wing loading, thrust-to-weight ratio, and stabilizer volume ratios held constant.

The re-sizing process terminates when the changes in the vehicle gross weight and subsystem weights between successive iterations are each smaller than a specified tolerance.

7. **Post-processing analyses:** This is a customizable module depending on the type of analysis being performed, and may include different means for data tabulation or visualization.

III.A. Brief Overview of ISSAAC Subsystem Modules

The subsystems considered within ISSAAC are divided into two groups, as shown in Fig. 3, which are evaluated in the following order:

1. Power consuming subsystems: which consume secondary power in pneumatic, hydraulic, or electric form and provide necessary functionality to the aircraft

2. Power generation and distribution subsystems: which are responsible for generation of secondary power, its transformation/regulation, and its distribution to the power consumers

For each subsystem considered, the end goal of the modeling approach is to identify the impacts along the four avenues shown in Fig. 2(b): (i) weight w_{sub}, (ii) shaft-power requirement $P_{spx}(t)$, (iii) bleed air requirement $\dot{m}_b(t)$, and (iv) direct drag increment $\Delta C_D(t)$ (the latter three may or may not be present, depending on the subsystem).

The connectivity among prime movers, power sources, power systems, and power consumers within an architecture (Fig. 2(a)) is determined automatically by an architecture definition algorithm. Using heuristic rules identified from inspection and extrapolation of the subsystem architectures of existing conventional aircraft and MEA, this algorithm rapidly determines a feasible connectivity among architecture components. Prior work[27] showed this to be equivalent to (or more conservative than) those present in existing commercial aircraft from a redundancy standpoint.

The Flight Controls Actuation System (FCAS) uses flight control surface definitions that are relative to the lifting surfaces. Sizing actuation loads for hinged control surface (ailerons, elevators, rudder, and spoilers) are computed using hinge moment coefficients[28] and relevant constraining flight conditions.[29,30] Actuating power requirements within a mission are estimated using the hinge moment coefficients and assumed control surface duty cycles.[31] Actuating power requirements for the high-lift devices and trimmable horizontal stabilizer are estimated using relationships between these quantities and aircraft maximum takeoff mass

SPX: shaft-power extraction
BX: bleed (air) extraction

MPGDS: Mechanical power generation & distribution (sub)system
HPGDS: Hydraulic power generation & distribution (sub)system
EPGDS: Electric power generation & distribution (sub)system
PPGDS: pneumatic power generation & distribution (sub)system

FCAS: Flight controls actuation (sub)system
LGAS: Landing gear actuation (sub)system
NWSS: Nose-wheel steering (sub)system
WBS: Wheel braking (sub)system
TRAS: Thrust reverser actuation (sub)system
ECS: Environmental control (sub)system
WIPS: Wing ice protection (sub)system
CIPS: Cowl ice protection (sub)system

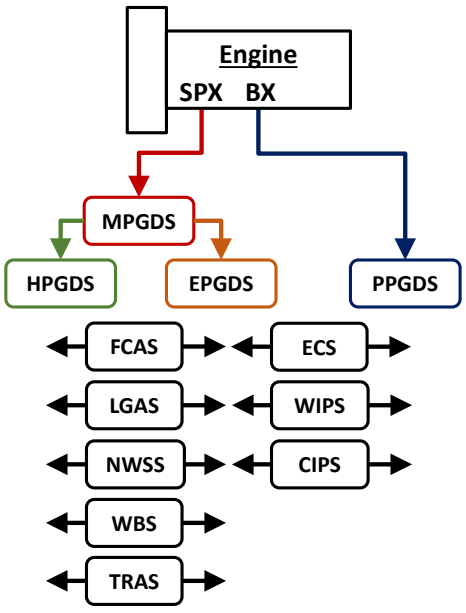

Figure 3. *Power consuming* and *power generation and distribution* subsystems considered

Table 1. Definition of Actuation Function Packages (AFPs) for FCAS, LGAS, NWSS, WBS, & TRAS

Actuation Function	Actuation Function Package (AFP) # (Electrification indicated by ✓or electric actuator type)							
	AFP-0	AFP-1	AFP-2	AFP-3	AFP-4	AFP-5	AFP-6	AFP-7
TRAS		✓	✓	✓	✓	✓	✓	✓
WBS		✓	✓	✓	✓	✓	✓	✓
LGAS			✓	✓	✓	✓	✓	✓
NWSS			✓	✓	✓	✓	✓	✓
FCAS-HLD				✓	✓	✓	✓	✓
FCAS-Sp.				EHA	EMA	EMA	EMA	EMA
FCAS-THSA					✓	✓	✓	✓
FCAS-Prim.						H/EHA	EHA	EMA

that were developed using published data for existing aircraft.[32–35] Estimates of the mass properties of the landing gears and a simplified model of the retraction/extension kinematics[36] are used to compute the actuation requirements for the Landing Gear Actuation System (LGAS). Nose-wheel Steering System (NWSS) actuation power requirement is computed based on gear geometry and critical loading conditions that generate maximum steering moments.[36,37] Predicted loads showed reasonable agreement with published loads from the ELGEAR project[38] (for Airbus A320 aircraft). Wheel Braking System (WBS) actuation requirements are computed using constraining static and dynamic braking cases.[30,36,39] Thrust reverser power requirements are expressed using a relationship that relates required power linearly to rated sea-level static engine thrust, which was developed using limited available data.[35,40] For each of these systems, the hydraulic or electric actuator masses are determined based on the actuation load/power that they are sized for. The presence of multiple actuation functions and multiple actuator designs results in a very large number of overall actuation architecture possibilities. Considering both computational tractability and the industry's demonstrated conservatism regarding electrification of actuation functions, it is assumed that they are electrified in a staged or *packaged* approach through a limited number of *Actuation Function Packages* (AFPs) AFP-0,..., AFP-7, as shown in Table 1. The successive actuation packages AFP-0,..., AFP-7 involve electrification of progressively more flight-critical actuation functions.

The ECS power requirement and drag generation are estimated based on (i) a cabin thermal analysis that accounts for internal heat loads and heat transfer between the cabin and the ambient across the cabin wall and (ii) a thermodynamic model of the ECS pack to compute the required mass flow rate of cooling ram air. To reduce case run time, the pack thermodynamic model is first evaluated off-line in order to create a gridded interpolant that relates required ram air mass flow with flight condition, pack air entry condition, and pack discharge temperature. This meta-model (and not the original pack model) is then queried during the mission performance evaluation. For electric ECS, mass additions from the cabin air compressors, electric motors, and their associated power electronics (which are driven by the electric pressurization power requirements) are accounted for.[20] Predicted power requirements compared well with published estimates for electric pressurization,[41] when reduced to a power-per-occupant basis.

The heating requirements for the Wing Ice Protection System (WIPS) and Cowl Ice Protection System (CIPS) are computed based on the protected surface area (defined parametrically with respect to the parent surface, i.e., the wing or the nacelle) and the necessary heat flux for a given flight and atmospheric condition.[20] These are computed using only limited geometric information about the aircraft's protected area. However, it was shown by other authors[42] that even such an approach provided acceptable estimates of the IPS power requirements for the Boeing 787 aircraft. The IPS mass is computed using a mass/length figure for pneumatic IPS and a mass/area figure for electrothermal IPS.

For hydraulic, pneumatic, and electric power generation and distribution systems (HPGDS, PPGDS, and EPGDS respectively), the masses of the power distribution elements (respectively hydraulic pipes, pneumatic ducts, and electric cables) are computed by (i) determining their existence and lengths from the architecture connectivity and the geometric model of the aircraft, and (ii) determining the mass-per-unit-length based on consideration of pressure drop, pressure, and voltage drop respectively. For the HPGDS and EPGDS, power sources (hydraulic pumps and electric generators respectively) are sized through the identification of

constraining flight conditions that require the maximum output from these components.[20] Their masses are then calculated from power-to-mass ratios identified from product data-sheets.

IV. Proposed Approach

IV.A. Formulating the Optimization Problem

In this work, the problem of simultaneously sizing and optimizing the aircraft and also sizing some major subsystems is posed as a multi-objective optimization statement. As mentioned previously, a number of objectives or objective functions have been considered in prior optimization studies in literature, the choice largely depending on the specific goals of the studies. Since the goal of this work is to analyze the effect of novel subsystem architectures on aircraft performance, *take-off field length* (TOFL), and *block fuel* (BF) are chosen as the objective functions. Take-off field length may be viewed as a surrogate for airport accessibility, and therefore is of interest to commercial airline carriers. Block fuel, on the other hand, is an indicator of fuel efficiency for a given design range. The rationale for choosing only two objectives is to simplify visualization and comparison of designs on different Pareto fronts.

The choice of design variables in a conceptual design study is usually motivated by the following: (i) designers should have access to them, and (ii) they should affect the aerodynamics, propulsion, and structures

Table 2. Continuous and discrete design variable ranges

	Range	
Design Variables	**SSA**	**LTA**
Thrust-to-weight ratio (TWR)	[0.25, 0.35]	[0.25, 0.35]
Wing loading (WSR, lb/ft^2)	[120, 135]	[115, 135]
Quarter-chord sweep (SWEEP, deg)	[25, 40]	[30, 40]
Thickness-to-chord ratio (TCA)	[0.05, 0.13]	[0.05, 0.13]
Taper ratio (TR)	[0.1, 0.4]	[0.1, 0.4]
Aspect ratio (AR)	[8, 12]	[10, 15]
Actuation function package (AFP)	{0, 1, . . . , 7}	{0, 1, . . . , 7}
Wing ice protection system (WIPS)	{0, 1, 2, 3}	{0, 1, 2, 3}
Cowl ice protection system (CIPS)	{0, 1, 2, 3}	{0, 1, 2, 3}
Environmental control system (ECS)	{0, 1}	{0, 1}

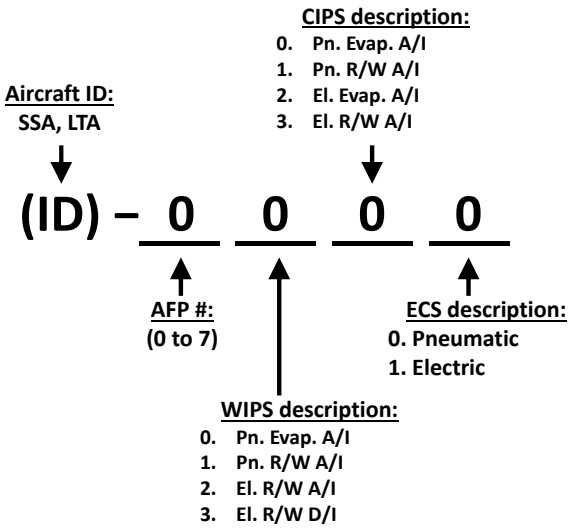

Figure 4. Subsystem architecture descriptor featuring discrete design variables

disciplines in an obvious, estimable, and significant manner. Thus, thrust-to-weight ratio (TWR), wing loading (WSR), wing quarter chord sweep (SWEEP), wing thickness-to-chord ratio (TCA), wing taper ratio (TR), and wing aspect ratio (AR) are chosen as the aircraft-level design variables. These are continuous design variables, which may take any value within defined upper and lower bounds (shown in Table 2).

The subsystem architectures, on the other hand, are described by discrete design variables (shown in Fig. 4) that denote the overall solutions employed for each subsystem. The first digit represents the Actuation Function Package (AFP), described in Table 1. The second and third digits describe the WIPS and CIPS solutions. These may differ in the secondary power type used (pneumatic vs. electric), the magnitude of supplied heat flux (in evaporative systems, the heat supplied is sufficient to completely evaporate impinging water, unlike in running-wet systems), and in the mode of operation (anti-ice systems operate continuously to prevent ice formation, while de-ice systems activate periodically to dispatch ice buildup). The fourth digit describes whether the ECS is of a conventional pneumatic type, which uses bleed air from the engines for cabin pressurization, or an electric solution which uses electrically driven compressors to compress ram air. Table 2 shows the discrete values that the subsystem architecture descriptor variables may take.

The optimization is subject to the following constraints, each of which is cast as a $\leq$-type constraint: (i) maximum TOFL (7,500 ft for both SSA and LTA), (ii) maximum wingspan (118 ft for SSA, 214 ft for LTA), (iii) positive excess fuel capacity, (iv) positive excess thrust (thus, climb gradient) for one-engine inoperative missed approach (AMFOR) (v) positive excess thrust (thus, climb gradient) for one-engine inoperative second segment climb (SSFOR), and (vi) maximum landing approach speed ($\text{VAPP}_{\max}$, 150 kt for both SSA and LTA). Side constraints corresponding to the upper and lower bounds of continuous design variables and the permissible values of discrete design variables are listed in Table 2. The optimization problem may now be formally stated as follows:

$$
\begin{aligned}
\underset{\mathbf{x}}{\text{minimize}} \quad & \mathbf{f}(\mathbf{x}) = \begin{bmatrix} \text{TOFL}(\mathbf{x}) \\ \text{BF}(\mathbf{x}) \end{bmatrix} \\
\text{subject to} \quad & \text{TOFL}(\mathbf{x}) - \text{TOFL}_{\text{baseline}} \leq 0, \\
& \text{Span}(\mathbf{x}) - \text{Span}_{\max} \leq 0, \\
& \text{Required fuel}(\mathbf{x}) - \text{Fuel capacity}(\mathbf{x}) \leq 0, \\
& -\text{AMFOR}(\mathbf{x}) \leq 0, \\
& -\text{SSFOR}(\mathbf{x}) \leq 0, \\
& \text{VAPP}(\mathbf{x}) - \text{VAPP}_{\max} \leq 0, \\
& \mathbf{x} : [\text{TWR, WSR, SWEEP, TCA, TR, AFP, WIPS, CIPS, ECS}]^T \in [\text{Table 2 intervals}]
\end{aligned}
$$

As the optimizer varies the design variables during the optimization, there may be combinations of design variables that fail to yield converged designs or result in errors thrown by ISSAAC modules or by FLOPS. Such situations, once detected, are handled by artificially appending high values to the objective functions (orders of magnitude higher than those for converged cases). This ensures that such designs are not carried forward into subsequent generations. Rather than finding a single optimum, the aim of this multi-objective optimization is to obtain Pareto-efficient designs in terms of the chosen objectives.

IV.B. Optimization Workflow

To perform the optimization described in the preceding section, the ISSAAC framework was integrated with the NSGA-II algorithm with the input/output interfaces depicted in Figure 5. The NSGA-II algorithm generates combinations of design variables (both continuous aircraft-level variables and discrete subsystem architecture descriptors) and queries ISSAAC, which performs the aircraft and subsystem sizing as well as the mission performance evaluation and returns values of the objectives and constraints to the optimization algorithm that correspond to the design variables.

On average, one evaluation costs $\mathcal{O}[40]$ seconds on a 3.40 GHz Intel i7 CPU with 16 GB of DDR3 RAM. For a high number of function calls (typically the case for evolutionary optimizers), this can result in intractable run times. Therefore, in order to reduce run time, queries to ISSAAC are parallelized. Thus, when the optimizer requires a set of candidates to be evaluated to determine their objectives and constraints, the work is split into different *workers* (processes), enabling simultaneous independent evaluations.

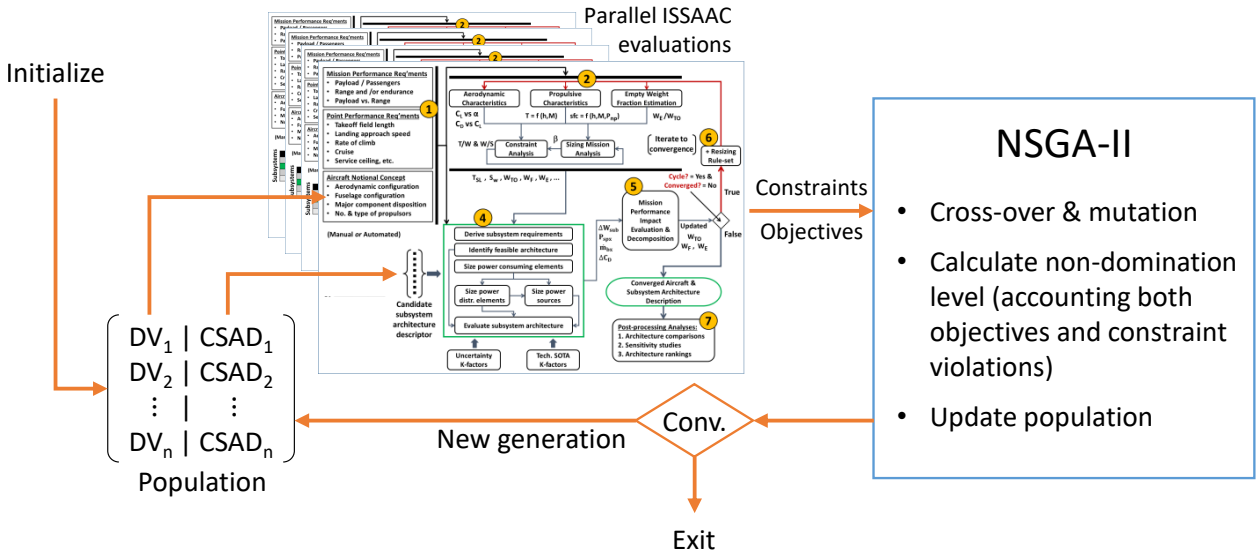

Figure 5. Optimization workflow depicting interfaces between the NSGA-II optimizer and the ISSAAC framework

Table 3. Data summary for reference Small Single-aisle Aircraft (SSA-0000), and Large Twin-aisle Aircraft (LTA-0000)

	Aircraft Identity	
Aircraft data	**SSA**	**LTA**
Passenger capacity	160	242
Design range (NM)	3,140	7,355
Cruise Mach number	0.780	0.850
Sea-level static thrust (lbf)	2 x 28,406	2 x 78,839
Wing planform area (ft^2)	1,411	4,061
Wingspan (ft)	118.0	217.4
Wing taper ratio	0.104	0.103
Wing 1/4-chord sweep (deg)	27.7	36.5
HT planform area (ft^2)	361	740
HT aspect ratio	6.27	5.22
HT taper ratio	0.203	0.243
HT 1/4-chord sweep (deg)	29.9	36.6
VT planform area (ft^2)	296	497
VT aspect ratio	1.92	1.80
VT taper ratio	0.276	0.327
VT 1/4-chord sweep (deg)	35.0	40.6
Fuselage length (ft)	124.8	183.4
Fuselage max. width (ft)	12.3	18.9
Fuselage max. height (ft)	13.2	19.4

IV.C. Establishing Reference Conventional Architecture Designs

To assess the effect of subsystem architectures on aircraft performance, two aircraft sizes are considered: (i) Small Single-aisle Aircraft (SSA) - similar to the Boeing 737-800, (ii) a Large Twin-aisle Aircraft (LTA) - similar to the Boeing 787-8. For both the aircraft classes, an optimization is first performed over only the aircraft-level continuous design variables with the subsystem architecture descriptors set to a conventional architecture (i.e., SSA-0000 and LTA-0000, see Fig. 4). The objective of this smaller-scale optimization problem is to establish a reference Pareto frontier to facilitate relative comparison of other subsystem architectures. From this Pareto frontier, the utopia point, defined as the hypothetical point that has the minimum of both objectives, is identified. Then, the design on the Pareto frontier that is closest to the utopia point (in the space of objectives) is chosen as a reference design. Since the objectives are physically different quantities, they are first normalized by their range prior to distance (norm) computations for all designs on the reference Pareto frontier. Figure 6 shows a graphical representation of the procedure used to establish the reference baseline (summarized in Table 3) and corresponding objective function values BF_{ref} and TOFL_{ref}. The BF and TOFL performance of all designs are expressed subsequently as percentage-deltas (%Δ), which are computed as $\%\Delta\mathrm{BF} = 100 \cdot (\mathrm{BF} - \mathrm{BF}_{ref})/\mathrm{BF}_{ref}$, $\%\Delta\mathrm{TOFL} = 100 \cdot (\mathrm{TOFL} - \mathrm{TOFL}_{ref})/\mathrm{TOFL}_{ref}$.

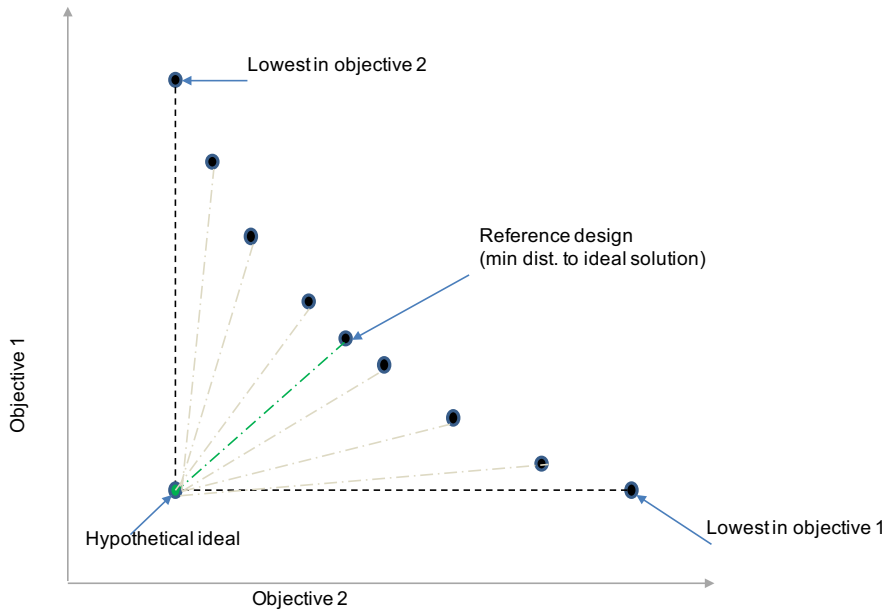

Figure 6. Visualization of the reference baseline

V. Results

For the smaller-scale optimization problem used to establish the reference SSA-0000 and LTA-0000 designs, a population size of 80 was used. For the larger-scale optimization with all continuous and discrete design variables, a population size of 100 was used. It was found that the choice of a population size of 80-100 members for optimization resulted in a dense sampling on the Pareto frontier. All the points are retained on the converged Pareto frontier. However, to ensure that they are truly non-dominated, the final population of designs is subject to a Pareto filter. The results are discussed in the following sections.

V.A. Small Single-Aisle Aircraft (SSA)

Figure 7 shows the movement of the SSA optimization's Pareto frontiers and also the composition of subsystem architectures (in percentages) with successive generations. The magnitude of improvement between generations (with respect to the BF and TOFL objective functions) reduces significantly as the optimization progresses. An interesting observation is the fact that electric ECS solutions (ECS descriptor = 1) feature in 100% of the populations from very early generations onward. This is due to fact that despite the increased shaft-power off-takes and component mass for electric ECS, the elimination of bleed air off-takes results in a

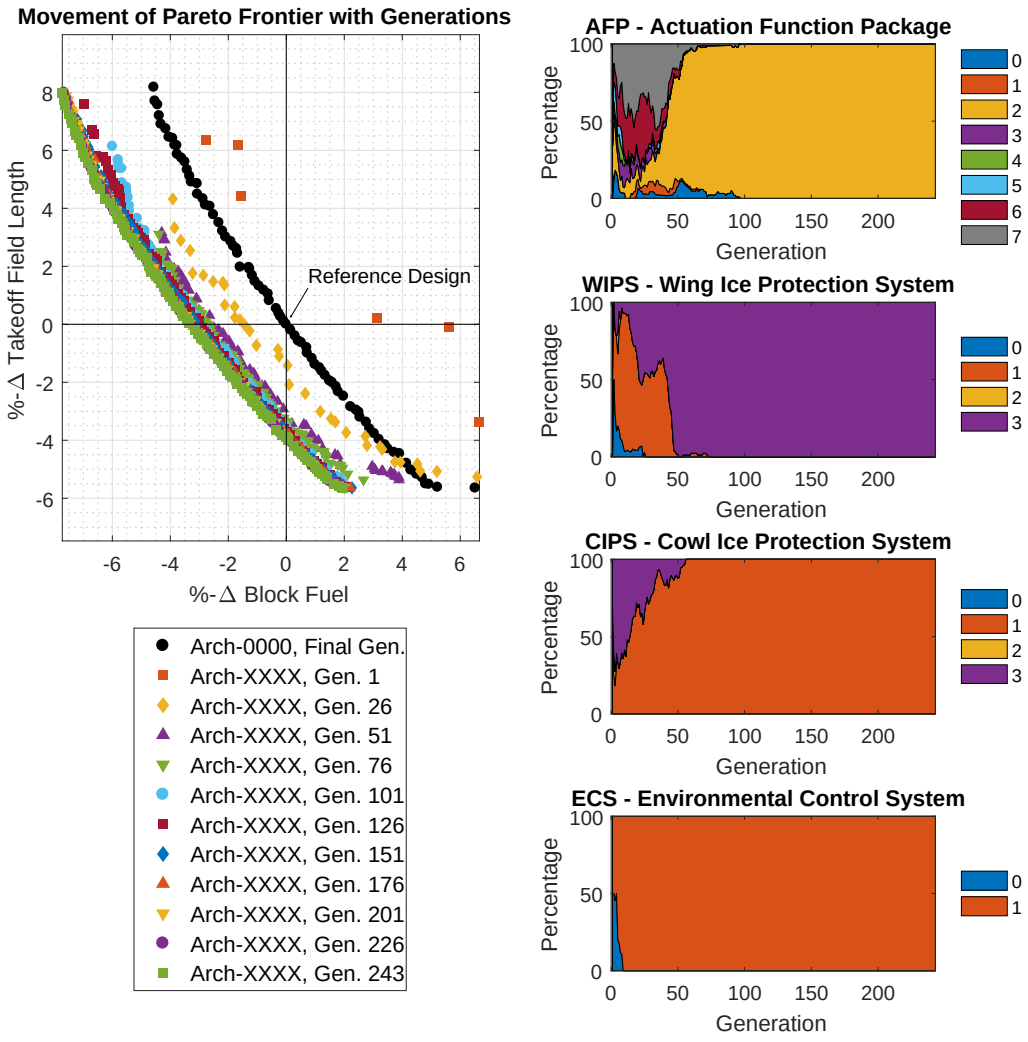

Figure 7. Evolution (over generations) of SSA BF, TOFL, and architecture compositions on Pareto Frontiers

net fuel burn benefit. At roughly the 80th generation mark, the WIPS solution converges to electrothermal running-wet de-icing system (WIPS descriptor = 3), while the CIPS converges to a pneumatic running-wet anti-icing solution (CIPS descriptor = 1). For the actuation functions, the last 30 generations show a roughly constant majority of designs with AFP#-2 (electric actuation for TRAS, WBS, LGAS, and NWSS), and a minority of designs with AFP#-7 (all electric EMA-based actuation).

It should be noted that the sizing problems at both the aircraft and subsystem levels are subject to epistemic uncertainty, and furthermore the subsystem-level problem is greatly affected by assumptions regarding technological state-of-the-art. Conclusions based solely on the characteristics of the final generation's Pareto frontier must, therefore, be avoided. Figure 8 shows the variation of both continuous and discrete design variables over a *Pareto band*, which includes the final generation's Pareto frontier as well as designs from prior generations which are not significantly worse-performing. The Pareto band in question was created using a 0.5% "look-back" for both the BF and TOFL objective functions. It is evident that designs with higher thrust-to-weight ratio (TWR) perform better with respect to TOFL but worse with respect to BF. Higher aspect ratio (AR) designs also perform better with respect to BF. The variation of the remaining continuous design variables among the designs within the Pareto band is not very significant.

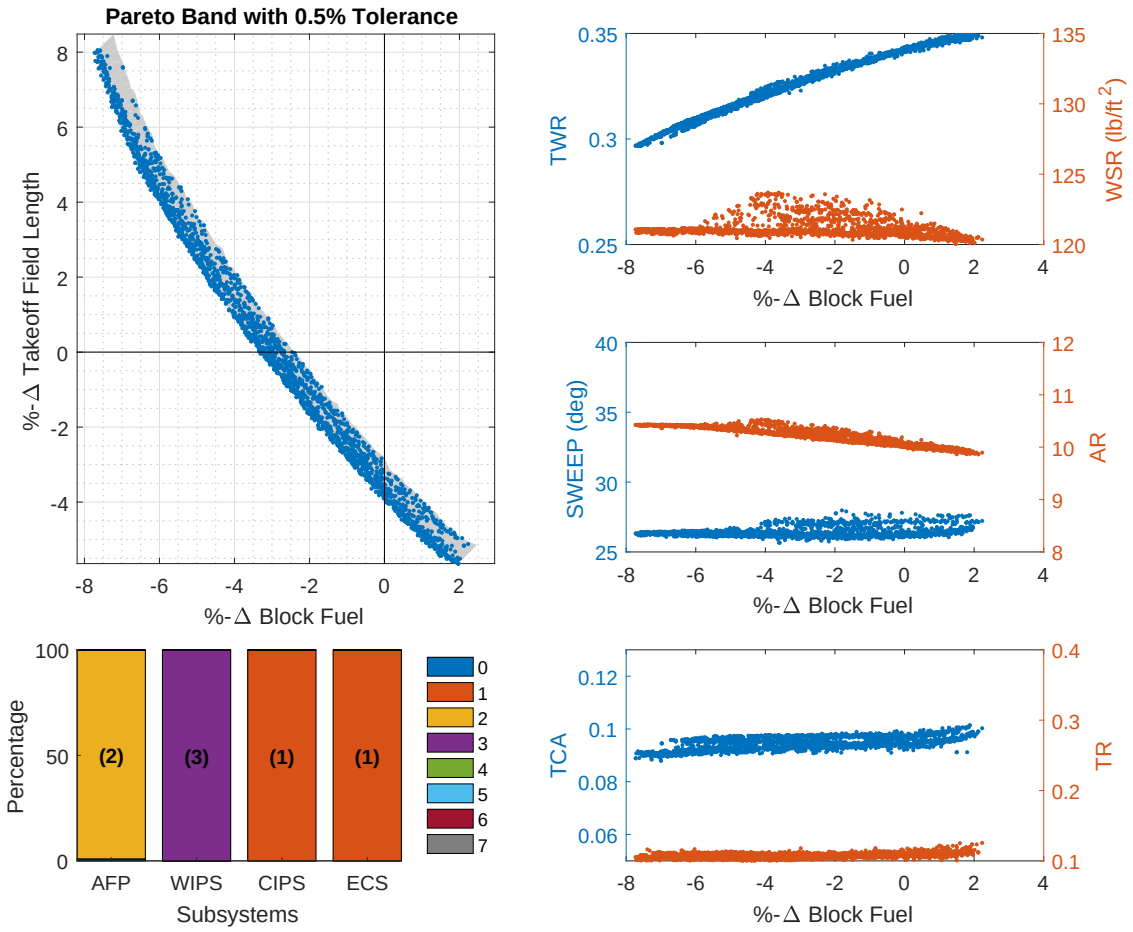

Figure 8. Variation of SSA continuous and discrete design variables within Pareto band

The trends observed with regard to composition of subsystem architectures within the Pareto band are strongly influenced by the modeling of the thrust-specific fuel consumption (TSFC) penalties arising out of shaft-power and bleed air extraction, which are dependent on the engine cycle parameters. However, in the current approach, the secondary power extraction penalties are estimated using a simpler approach where the incremental fuel flow $\Delta\dot{w}_{f,spx}$ per engine due to total shaft-power extraction of P_{spx} is modeled based on the k_p^* approach of Scholz[43] as

$$\Delta\dot{w}_{f,spx} = \dot{w}_{f,0}\ k_p^*\ \frac{P_{spx}[kW]}{N_{op,eng}\ T_{SL}[kN]}, \qquad \text{(per engine)} \tag{2}$$

in which $\dot{w}_{f,0}$ is the basic fuel flow rate (without shaft-power extraction) for each of $N_{op,eng}$ engines which are assumed to contribute equally to the total shaft-power P_{spx}. The constant k_p^* was given as $k_p^* = 0.0094$ N/W as an average of the penalties computed at flight altitudes of 0 ft, 10,000 ft, 20,000 ft, and 35,000 ft at Mach numbers of 0.30, 0.60, and 0.85 at maximum continuous thrust.[43] The incremental fuel flow $\Delta\dot{w}_{f,bx}$ due to bleed air extraction $\dot{w}_{bld} = \dot{m}_{bld} \cdot g$ per engine is computed following the method of SAE AIR 1168/8[44] as

$$\Delta\dot{w}_{f,bx} = 0.0335\ \left(\frac{T_{tet}[^\circ R]}{2000}\ \frac{\dot{w}_{bld}}{N_{op,eng}}\right), \qquad \text{(per engine)} \tag{3}$$

in which T_{tet} is the turbine entry temperature, for which a representative value of 2,400°R is used in this paper. Off-take penalty relationships such as Eq. 2 and Eq. 3 are useful as they require little information other

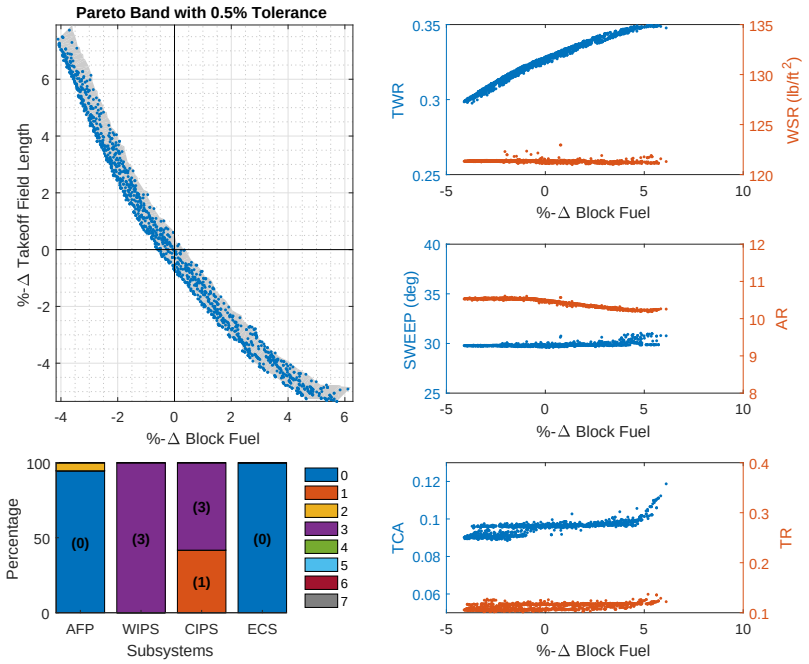

Figure 9. Variation of SSA continuous and discrete design variables within Pareto band, $\kappa_{spp} = 0.3$

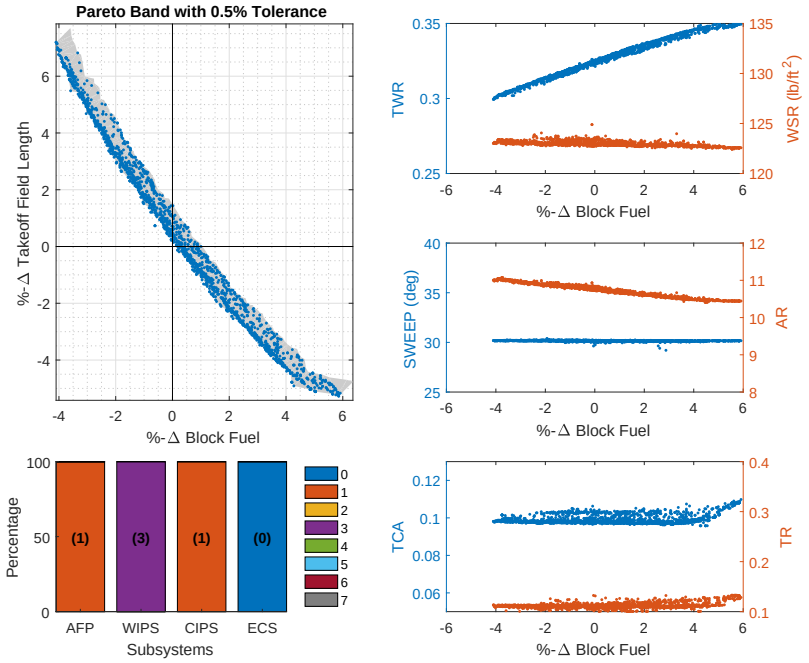

Figure 10. Variation of SSA continuous and discrete design variables within Pareto band, $\kappa_{spp} = 0.5$

than the time variation of the shaft-power and bleed air off-takes. They are, however, general relationships that do not account for the effect of the engine cycle parameters on the engine's sensitivity to secondary power extraction. The effect of this uncertainty on the performance of a substantially electrified subsystem architecture relative to a conventional one is assessed through a factor κ_{spp} that modifies the secondary power extraction penalty relationships shown above. Of particular interest is a case where shaft-power extraction is *more* expensive than predicted by Eq. 2 and bleed extraction is *less* expensive than predicted by Eq. 3. This scenario is modeled as follows: (i) the factor κ_{spp} is constrained as $\kappa_{spp} \geq 0$, (ii) the RHS of Eq. 2 is multiplied by the quantity $(1 + \kappa_{spp})$, and (iii) the RHS of Eq. 3 is multiplied by the quantity $(1 - \kappa_{spp})$.

From Fig. 9 ($\kappa_{spp} = 0.3$) and Fig. 10 ($\kappa_{spp} = 0.5$), it is evident that the results, in terms of architecture composition, are very sensitive to the secondary power extraction penalties. If shaft-power off-take becomes relatively more expensive and bleed air off-take simultaneously becomes relatively less expensive, a pneumatic ECS solution is favored across the entire population. With $\kappa_{spp} = 0.5$, the CIPS solution is affected as well. As a secondary effect or consequence, the composition of AFP packages also changes to show a greater proportion of less electrified actuation solutions. Another important observation is that trends in the aircraft-level continuous design variables for the non-dominated solutions remain largely unchanged, implying that the subsystem architecture has a somewhat more significant impact on the objectives for these scenarios.

V.B. Large Twin-Aisle Aircraft

Figure 11 shows the movement of the LTA Pareto frontiers and the composition of subsystem architectures (in percentages) with successive generations. It is evident that non-dominated population is entirely com-

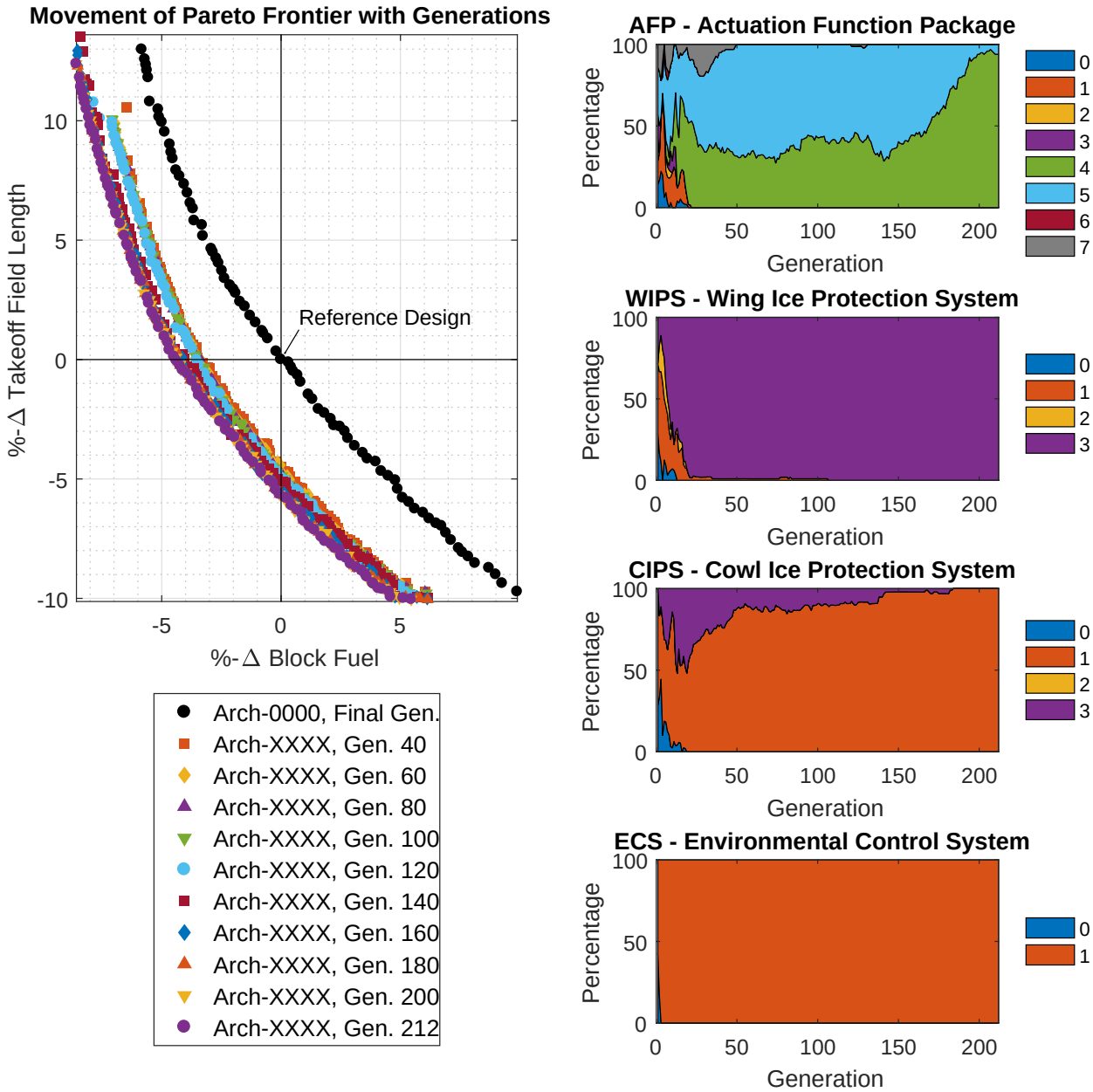

Figure 11. Evolution (over generations) of LTA BF, TOFL, and architecture compositions on Pareto Frontiers

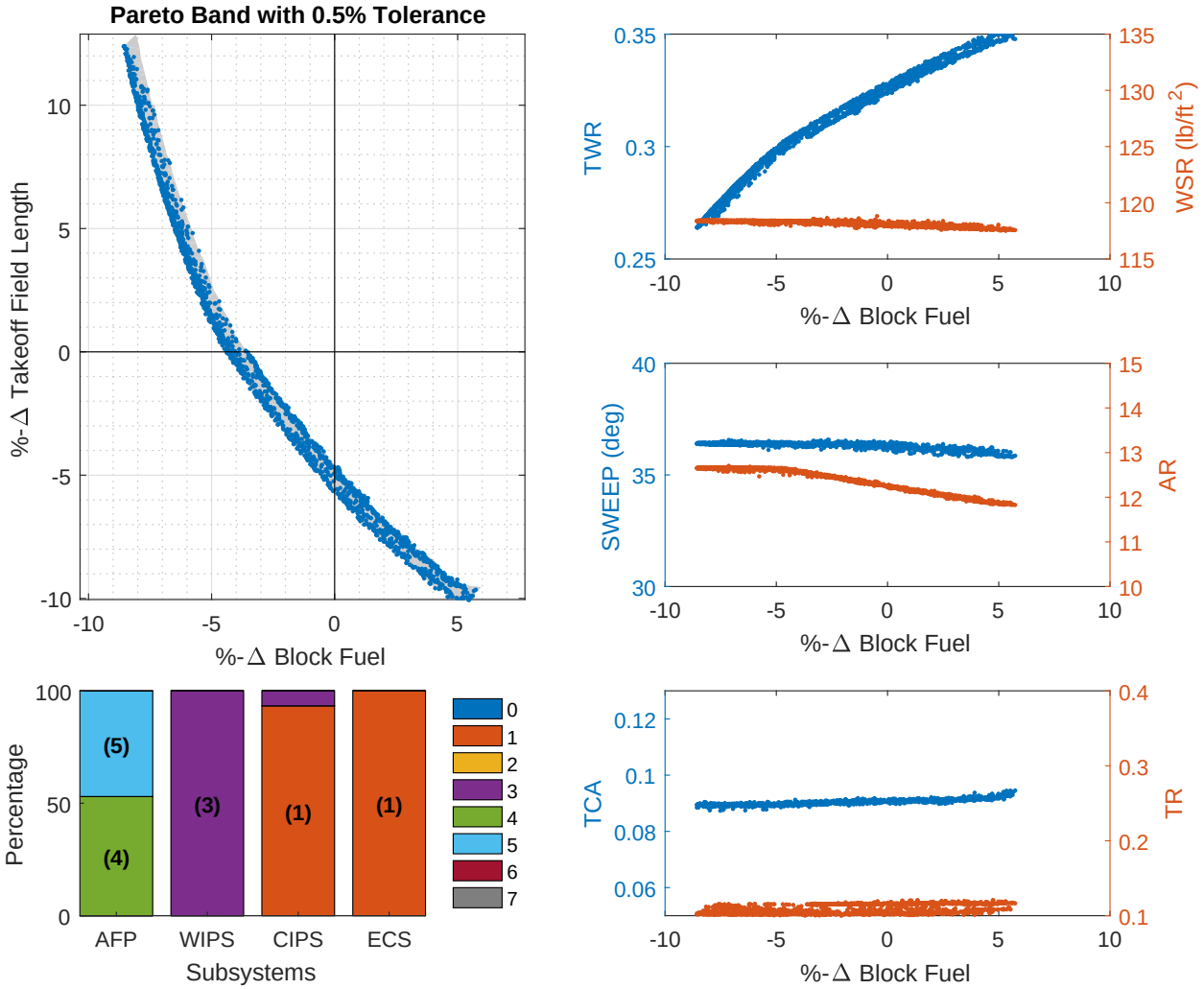

Figure 12. Variation of LTA continuous and discrete design variables within Pareto band

posed of fully electric actuation (AFP#-7), electrothermal running-wet de-icing WIPS (WIPS descriptor = 3), pneumatic running-wet anti-icing CIPS (CIPS descriptor = 1), and electric ECS (ECS descriptor = 1). Similar to the case of the SSA, the architecture of dominant LTA solutions get frozen in the earlier generations, with most of the optimization in later generations being driven by the aircraft-level continuous design variables. Therefore, as seen from Fig. 12, the Pareto band resulting from a 5% look-back does not show much architectural diversity.

When the impact of secondary power extraction penalties is assessed with a setting of $\kappa_{spp} = 0.35$, as shown in Fig. 13, the ECS is still electric (ECS descriptor = 1). However, when it is increased to $\kappa_{spp} = 0.5$, the ECS architecture reverts to pneumatic throughout the Pareto band (ESC descriptor = 0), as depicted in Fig. 14. These observations imply that the LTA aircraft is relatively less sensitive to the factor κ_{spp}. This is due to the comparatively larger contribution of ECS bleed air off-take to the total fuel impact for the larger, longer-range LTA.

VI. Conclusion and Future Work

This work presented a multi-objective constrained optimization approach for aircraft sizing taking into account the impact of the major aircraft subsystems. The approach uses the Non-Dominated Sorting Algorithm II (NSGA-II) to harness the Integrated Subsystem Sizing and Architecture Assessment Capability (ISSAAC) framework, using both continuous design variables for key aircraft-level design parameters and

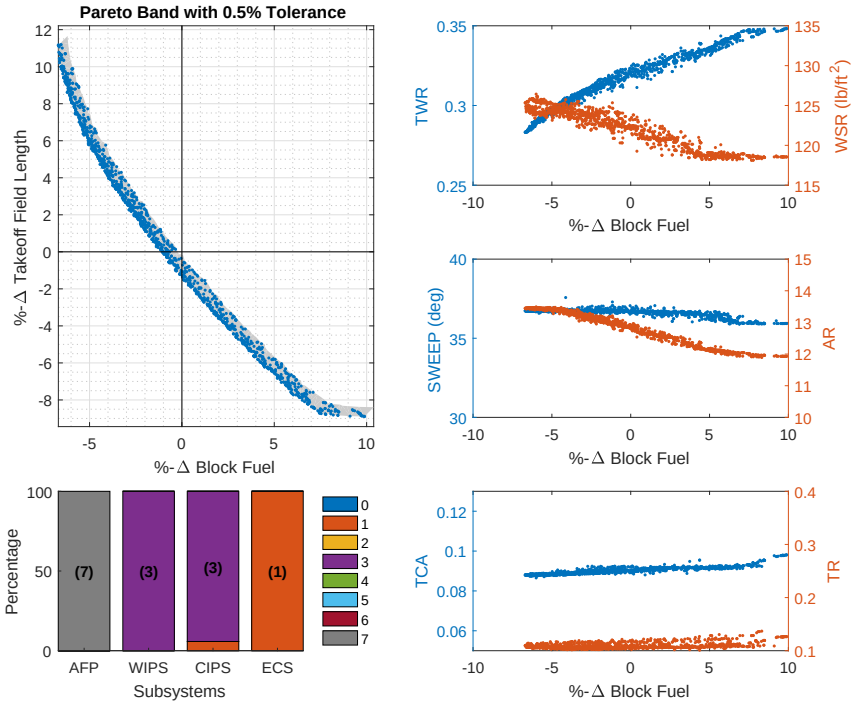

Figure 13. Variation of LTA continuous and discrete design variables within Pareto band, $\kappa_{spp} = 0.35$

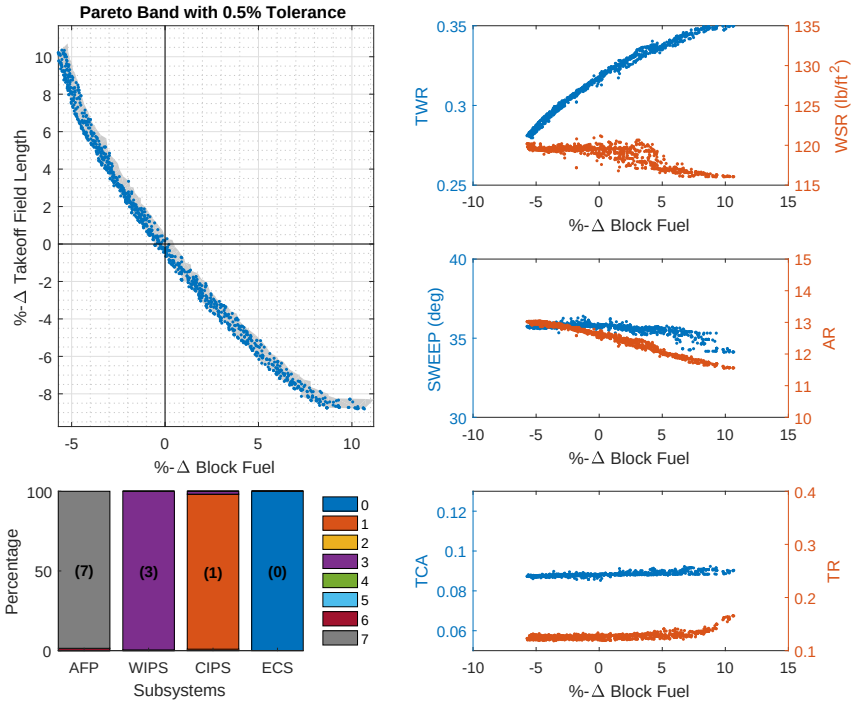

Figure 14. Variation of LTA continuous and discrete design variables within Pareto band, $\kappa_{spp} = 0.5$

discrete variables as subsystem architecture descriptors. For both a Small Single-aisle Aircraft (SSA) and a Large Twin-aisle Aircraft (LTA), successive generations revealed the evolution of architecture composition on the Pareto frontier towards a small number of dominant subsystem architectures. For both aircraft, these architectures involved electrification of the Environmental Control System (ECS), which occurred in early generations of the optimization and had a significant impact. Electrothermal de-icing solutions for the Wing

Ice Protection System (WIPS) were also found to be dominant, while pneumatic running-wet anti-icing solutions dominated for the Cowl Ice Protection System (CIPS). The dominant architectures for the two aircraft sizes showed varying levels of electrification for the actuation functions. The architecture composition within the Pareto bands (generated by a look-back starting from the final Pareto frontiers) changed significantly when the magnitudes of thrust-specific fuel consumption degradation arising from shaft-power and bleed air extraction were varied in opposite directions. In particular, when shaft-power extraction was made relatively more expensive and bleed air extraction relatively less expensive, the electrification trends observed for ECS, in particular, were reversed. Avenues for future work include (i) formulation of a larger scale optimization problem with optimization performed for the subsystems as well, and (ii) a formal assessment of the impact of epistemic and technological uncertainty on the results of such multi-objective optimization problems.

References

[1]Henderson, R. P., Martins, J., and Perez, R. E., "Aircraft conceptual design for optimal environmental performance," *Aeronautical Journal*, Vol. 116, No. 1175, 2012, pp. 1.

[2]Antoine, N. E. and Kroo, I. M., "Framework for aircraft conceptual design and environmental performance studies," *AIAA journal*, Vol. 43, No. 10, 2005, pp. 2100–2109.

[3]Cabral, L. V., Paglione, P., and Mattos, B., "Multi-objective design optimization framework for conceptual design of families of aircraft," *44th AIAA Aerospace Sciences Meeting and Exhibit, Reno, Nevada*, 2006, pp. 2006–1328.

[4]Daskilewicz, M. J., German, B. J., Takahashi, T. T., Donovan, S., and Shajanian, A., "Effects of disciplinary uncertainty on multi-objective optimization in aircraft conceptual design," *Structural and Multidisciplinary Optimization*, Vol. 44, No. 6, 2011, pp. 831–846.

[5]Ilario da Silva, C. R., Orra, T. H., and Alonso, J. J., "Multi-Objective Aircraft Design Optimization for Low External Noise and Fuel Burn," *58th AIAA/ASCE/AHS/ASC Structures, Structural Dynamics, and Materials Conference*, 2017, p. 1755.

[6]Raymer, D., *Aircraft Design: A Conceptual Approach*, AIAA Education Series, 4th ed., 2006.

[7]Roskam, J., *Airplane Design Part V - Component Weight Estimation*, Design Analysis & Research, 1999.

[8]Torenbeek, E., *Synthesis of Subsonic Airplane Design: An Introduction to the Preliminary Design of Subsonic General Aviation and Transport Aircraft, with Emphasis on Layout, Aerodynamic Design, Propulsion and Performance*, Delft University Press, 1976.

[9]Jones, R., "The More Electric Aircraft: the past and the future?" *IEE Colloquium on Electrical Machines and Systems for the More Electric Aircraft*, 1999, pp. 1/1–1/4.

[10]Cronin, M., "The all-electric aircraft," *IEE Review*, Vol. 36, No. 8, sep 1990, pp. 309 –311.

[11]Sinnett, M., "Boeing 787 No-Bleed Systems: Saving Fuel and Enhancing Operational Efficiencies," Boeing Aero Magazine, Quarter 4, Online: `http://www.boeing.com/commercial/aeromagazine/`, 2007.

[12]Nelson, T., "787 Systems and Performance," Flight Operations Engineering, Boeing Commercial Airplanes, March 2009, online: `http://myhres.com/Boeing-787-Systems-and-Performance.pdf`, accessed November 4, 2015.

[13]Van den Bossche, D., "The A380 Flight Control Electrohydrostatic Actuators, Achievements and Lessons Learnt," *25th International Congress of the Aeronautical Sciences, ICAS 2006*, Hamburg, Germany, 2006.

[14]Chakraborty, I. and Mavris, D. N., "Integrated Assessment of Aircraft and Novel Subsystem Architectures in Early Design," *54th AIAA Aerospace Sciences Meeting*, 2016, p. 0215.

[15]Chakraborty, I. and Mavris, D. N., "Assessing Impact of Epistemic and Technological Uncertainty on Aircraft Subsystem Architectures," *16th AIAA Aviation Technology, Integration, and Operations Conference*, 2016, p. 3145.

[16]Lammering, T., *Integration of Aircraft Systems into Conceptual Design Synthesis*, Ph.D. thesis, Institute of Aeronautics and Astronautics (ILR), RWTH Aachen University, 2014.

[17]Chakraborty, I. and Mavris, D., "Integrated Assessment of Aircraft and Novel Subsystem Architectures in Early Design," *AIAA Science and Technology Exposition and Forum (SciTech)*, No. AIAA 2016-0215, San Diego, California, 4-8 January 2016.

[18]Deb, K., *Multi-objective optimization using evolutionary algorithms*, Vol. 16, John Wiley & Sons, 2001.

[19]Deb, K., Pratap, A., Agarwal, S., and Meyarivan, T., "A fast and elitist multiobjective genetic algorithm: NSGA-II," *IEEE transactions on evolutionary computation*, Vol. 6, No. 2, 2002, pp. 182–197.

[20]Chakraborty, I., *Subsystem Architecture Sizing and Analysis for Aircraft Conceptual Design*, Ph.D. thesis, Daniel F. Guggenheim School of Aerospace Engineering, Georgia Institute of Technology, Atlanta, GA, USA, Online: `https://smartech.gatech.edu/handle/1853/54427`, December 2015.

[21]Chakraborty, I. and Mavris, D. N., "Integrated Assessment of Aircraft and Novel Subsystem Architectures in Early Design," *Journal of Aircraft*, 2016, pp. 1–15.

[22]Sanchis, J., Martinez, M., Blasco, X., and Salcedo, J., "A new perspective on multiobjective optimization by enhanced normalized normal constraint method," *Structural and multidisciplinary optimization*, Vol. 36, No. 5, 2008, pp. 537–546.

[23]Messac, A., Ismail-Yahaya, A., and Mattson, C. A., "The normalized normal constraint method for generating the Pareto frontier," *Structural and multidisciplinary optimization*, Vol. 25, No. 2, 2003, pp. 86–98.

[24]Das, I. and Dennis, J. E., "Normal-boundary intersection: A new method for generating the Pareto surface in nonlinear multicriteria optimization problems," *SIAM Journal on Optimization*, Vol. 8, No. 3, 1998, pp. 631–657.

[25]McCullers, L., *Flight Optimization System, Release 8.11, User's Guide*, NASA Langley Research Center, Hampton, VA 23681-0001, October 9 2009.

[26]Lytle, J. K., "The Numerical Propulsion System Simulation: An Overview," NASA/TM-2000-209915, http://ntrs.nasa.gov/archive/nasa/casi.ntrs.nasa.gov/20000063377.pdf, June 2000.

[27]Chakraborty, I. and Mavris, D., "Heuristic Definition, Evaluation, and Impact Decomposition of Aircraft Subsystem Architectures," *AIAA Aviation 2016 Conference*, No. AIAA-2016-3144, Washington D.C., June 13-17, 2016.

[28]Roskam, J., *Airplane Design Part VI - Preliminary Calculation of Aerodynamic, Thrust and Power Characteristics*, Design Analysis & Research, 1999.

[29]Scholz, D., "Development of a CAE-Tool for the Design of Flight Control and Hydraulic Systems," *AeroTech '95*, Birmingham, U.K., 1995.

[30]"Federal Aviation Regulations (FAR) Part 25 - Airworthiness Standards: Transport Category Airplanes," Federal Aviation Administration (FAA), online: http://www.ecfr.gov/, accessed November 4, 2015.

[31]Simsic, C., "Electric actuation system duty cycles," *Aerospace and Electronics Conference, 1991. NAECON 1991., Proceedings of the IEEE 1991 National*, 1991, pp. 540–545 vol.2.

[32]*Boeing 777 Aircraft Maintenance Manual, Chapter 27 - Flight Controls*, 2006.

[33]Society of Automotive Engineers, "SAE Aerospace Information Report (AIR) 5005A - Commercial Aircraft Hydraulic Systems," 2010.

[34]Lammering, T., *Integration of Aircraft Systems into Conceptual Design Synthesis*, Ph.D. thesis, Institute of Aeronautics and Astronautics (ILR), RWTH Aachen University, 2014.

[35]Socheleau, J., Mare, J.-C., and Baudu, P., "Actuation Technologies and Application - Flight Controls and Thrust Reverser Actuation," *Technologies for Energy Optimized Aircraft Equipment Systems (TEOS forum)*, Paris, France, 2006.

[36]Chakraborty, I., Mavris, D., Emeneth, M., and Schneegans, A., "An Integrated Approach to Vehicle and Subsystem Sizing and Analysis for Novel Subsystem Architectures," *Proc IMechE Part G: J Aerospace Engineering*, Vol. 230, No. 3, 2016, pp. 496–514.

[37]Cameron-Johnson, A., "Some Aspects of the Design of Aircraft Steering Systems," *Aircraft Engineering and Aerospace Technology*, Vol. 43, No. 6, 1971, pp. 7–10.

[38]Bennett, J., Mecrow, B., Atkinson, D., Maxwell, C., and Benarous, M., "Fault-tolerant electric drive for an aircraft nose wheel steering actuator," *IET Electrical Systems in Transportation*, Vol. 1, No. 3, 2011, pp. 117–125.

[39]Collins, A., "EABSYS: Electrically Actuated Braking System," *IEE Colloquium on Electrical Machines and Systems for the More Electric Aircraft*, London, U.K., 1999, p. 4.

[40]Scholz, D., "MPC 75 Hydraulic Load Analysis," Technical Note TN-EV52-362/91, Deutsche Airbus, Hamburg, July 1991.

[41]Herzog, J., "Electrification of the Environmental Control System," *25th International Congress of the Aeronautical Sciences (ICAS)*, No. ICAS 2006-7.7.1, Hamburg, Germany, 3 - 8 September 2006.

[42]Meier, O. and Scholz, D., "A Handbook Method for the Estimation of Power Requirements for Electrical De-Icing Systems," *Deutscher Luft-und Raumfahrtkongress 2010*, Hamburg, Germany, Aug. 31 - Sept. 2 2010.

[43]Scholz, D., Seresinhe, R., Staack, I., and Lawson, C., "Fuel Consumption due to Shaft Power Off-takes from the Engine," *4th International Workshop on Aircraft System Technologies, AST 2013*, Shaker, Hamburg,, April 23-24 2013, pp. 169–179.

[44]Society of Automotive Engineers, "SAE Aerospace Applied Thermodynamics Manual - SAE AIR 1168," 1989.